BIOMOLECULES & THERAPEUTICS

Original Article
Biomol Ther 22(6), 503-509 (2014)

Paraquat Induces Apoptosis through Cytochrome C Release and ERK Activation

Hong Joo Seo[1], Sang Joon Choi[2] and Jung-Hee Lee[3,*]

[1]Department of Thoracic and Cardiovascular Surgery, [2]Department of Obstetrics and Gynecology, Chosun University Hospital, [3]Department of Cellular and Molecular Medicine, Chosun University School of Medicine, Gwangju 501-759, Republic of Korea

Abstract

Paraquat has been suggested to induce apoptosis by generation of reactive oxygen species (ROS). However, little is known about the mechanism of paraquat-induced apoptosis. Here, we demonstrate that extracellular signal-regulated protein kinase (ERK) is required for paraquat-induced apoptosis in NIH3T3 cells. Paraquat treatment resulted in activation of ERK, and U0126, inhibitors of the MEK/ERK signaling pathway, prevented apoptosis. Moreover, paraquat-induced apoptosis was associated with cytochrome C release, which could be prevented by treatment with the MEK inhibitors. Taken together, our findings suggest that ERK activation plays an active role in mediating paraquat-induced apoptosis of NIH3T3 cells.

Key Words: Paraquat, NIH3T3 cells, ERK1/2, Apoptosis, Cytochrome C, MAPK

INTRODUCTION

Paraquat, a redox-cycling compound, is a strong pneumotoxicant (Wallace *et al*., 2005). Paraquat is also able to induce behavioral and neurological disorders such as Parkinsonism (Mak *et al*., 2011; Prakash *et al*., 2013; Qin *et al*., 2014). The molecular mechanisms responsible for the cytotoxic effects of paraquat in cells are not fully understood but are mainly attribute to their ability to generation of reactive oxygen species (ROS) and subsequent interactions with intracellular marcromolecules such as lipids, proteins, and nucleic acids to trigger apoptosis (Rincheval *et al*., 2012; Chang *et al*., 2013; Wang *et al*., 2014c). Recent investigations have shown that paraquat induces apoptosis through mitochondria perturbation including cytochrome C release, subsequent caspase-3 and poly (ADP-ribose) polymerase cleavage (Hong *et al*., 2013; Han *et al*., 2014). Paraquat also induced expression of Bcl-2 family proteins such as Bak, Bid, BNip3 and Noxa, and can be triggered apoptosis through extrinsic and intrinsic cell death pathway (Fei and Ethell, 2008; Fei *et al*., 2008). However, many studies have demonstrated paraquat-induced apoptosis in various cells, but the detailed mechanism of paraquat-induced apoptosis remains largely unknown.

ROS have been shown to participate in the number of human diseases such as cancer, neurodegeration and aging (Li *et al*., 2013; Giordano *et al*., 2014; Kim *et al*., 2014; Meierjohann, 2014). Therefore, ROS have been generally considered to directly toxic to cell. However, recent studies have demonstrated that ROS play a role as second messengers to regulate mitogen-activated protein kinase (MAPK) in various cells (Son *et al*., 2013; Tormos *et al*., 2013), MAPK family constitutes important mediators of signal transduction processes. The ERK1/2 pathway is regulated mostly by mitogenic stimuli, and leads to the production of proteins required for cell growth and differentiation (Munshi and Ramesh, 2013; Liu *et al*., 2014). In contrast, JNK and p38 are activated primarily by various stresses and are involved in cell transformation, stress responses and apoptosis (Haberzettl and Hill, 2013; Lim *et al*., 2013; Darling and Cook, 2014; Tian *et al*., 2014b). Recently, some experiments have shown that paraquat-induced ROS production participates in the phosphorylation of p38, ERK or JNK MAPK (Miller *et al*., 2007; Ding *et al*., 2009; Wang *et al*., 2014c).

Although paraquat has been implicated as a ROS inducer, its mechanisms are largely unknown. In the present study, we investigated the mechanism of paraquat-induced apoptosis in NIH3T3 cells. The results demonstrate that although ERK, JNK, and p38 were all found to be activated in response to paraquat treatment, only ERK activity is important in mediating paraquat-induced apoptosis through a cytochrome C re-

Open Access **http://dx.doi.org/10.4062/biomolther.2014.115**

Received Oct 14, 2014 **Revised** Oct 25, 2014 **Accepted** Nov 4, 2014
Published online Nov 30, 2014

***Corresponding Author**
E-mail: jhlee75@chosun.ac.kr
Tel: +82-62-230-6399, Fax: +82-62-230-6751

lease-dependent mechanism.

MATERIAL AND METHODS

Reagents and antibodies

Paraquat (PQ), N-acetylcystein (NAC) and propidium iodide (PI) were purchased from Sigma (St. Louis, MO, USA). The MEK inhibitor (U0126), the p38 inhibitors (SB203580) and were all obtained from CalBiochem (San Diego, CA, USA). The anti-Cytochrome C antibody was purchased from Transduction Laboratories (Lexington, KY, USA). The Elk and ERK1/2 antibodies were from Cell signaling Technology (Beverly, MA, USA).

Cell cultures

The NIH3T3 mouse embryo fibroblast cell line was obtained from the ATCC (Manassas, VA, USA) and was maintained in Dulbecco's modified Eagle's medium supplemented with 10% fetal bovine serum, 2 mM L-glutamine, 100 units of penicillin/ml, and 100 μg of streptomycin/ml (Invitrogen, Carlsbad, CA, USA). They were cultured at 37°C in a humidified chamber containing 5% CO_2.

Plasmid constructs and oligonucleotides

pRL-Luc plasmid was purchased from Promega (San Diego, CA, USA). Gal4-cJun, Gal4-CHOP and Gal4-ElK1 plasmid were purchased from Stratagene (La Jolla, CA, USA). JNK antisense (AS) oligonucleotides used in this study were synthesized at ISIS Pharmaceuticals, Inc. (Carlsbad, CA, USA). The sequences of the oligonucleotides used are as follows: Control (ISIS 17552), TCAGTAATAGCCCCACATGG; JNK1 AS (ISIS 15347), CTCTGTAGGCCCGCTTGG; JNK2 AS (ISIS 15354), GTCCGGGCCAG-GCCAAAGTC. All oligonucleotides were 2'-O-methoxyethyl chimers containing five 2'-O-methoxyethyl-phosphodiester residues flanking a 2'-deoxynucleotide-phosphorothioate region (Bost *et al*., 1997).

Transfection and luciferase activity assay

To monitor MAPK activity levels, we used luciferase assay based on the fusion proteins that include GAL4 DNA binding domain fused to the activation domain of specific transfection factors that, in turn, drive the expression of *firefly* luciferase reporter gene. An expression plasmid encoding fusion protein GAL4-Elk (pFA-Elk for ERK activation), GAL4-CHOP (for p38 activation) or GAL4-c-Jun (for JNK activation) was used. In all transfection, a plasmid encoding *renilla* luciferase was co-transfected, and *firefly* luciferase activity was normalized to *renilla* luciferase activity. Dual luciferase activity in the cell extracts was determined according to manufacture's instruction (Promega, Madison, WI, USA). Briefly, each assay mixture contained 20 μl cell lysate and 100 μl luciferase measuring buffer (LAR II^R, Promega) and *Firefly* luciferase and *Renilla* luciferase activity was measured by luminometer (Glomax, Promega). The luciferase activity data were normalized to the *Renilla* value, and the results were represented as the average and standard deviation (S.D.) from triplicate of experiments.

PI staining

Cells were collected 24 h following treatment, fixed in 70% ethanol, and stained with propidium iodide (PI, 50 μg/ml) after RNA digestion. PI-stained 10,000 cells were analyzed for DNA content with a FACScan flow cytometer (Becton Dickinson, San Jose, CA, USA).

ERK kinase assay

The cells were lysed and sonicated in a buffer containing Tris (10 mm, pH 7.5), NaCl (150 mM), EGTA (2 mM), orthovanadate (1 mM), DTT (2 mM) and protease inhibitors: aprotinine (10 μg/ml), leupeptin (10 μg/ml) and phenylemethanesulfonyl fluoride (PMSF) (1 mM) for 30 min at 4°C. Activity was assessed using p44/42 MAP kinase assay kit (Cell Signaling Technology, Inc.). Briefly, the lysates were immunoprecipitated with immobilized phopho-p44/42 MAP kinase monoclonal antibody for 5 h at 4°C and the immune complexes were washed three times with lysis buffer, once with kinase buffer, and resuspended in kinase buffer containing Elk-1 fusion protein. The reactions were incubated for 30 min at 30°C and terinated by the addition of SDS sample buffer and analyzed by immunoblotting with anti-phopho-Elk-1 antibody and ERK1/2 antibody. The antigen antibody complexes were visualized by chemiluminescence (Amersham Pharmacia Biotech, Arlington Heights, IL, USA). Real time PCR analysis was performed for quantification of ERK using the Mx3000P (Stratagene, La Jolla, CA, USA).

Release of cytochrome C

Approximately 5×10^6 cells were trypsinized and collected by centrifugation and the resultant pellets were washed with PBS and resuspended in 100 μl buffer containing 250 mM sucrose, 20 mM HEPES, pH 7.5, 10 mM $MgCl_2$, 1 mM EDTA, 1 mM EGTA, 1 mM dithiothreitol and 1 mM PMSF. The cells were then homoginized with 15 strokes of a Teflon homogenizer on ice, and the resulting homogenates were centrifuged at 1000 g for 10 min at 4°C. The supernatants were further centrifuged at 15000 g for 20 min. The resulting supernatants were reserved as the cytosolic fraction and used for Western blot analysis with anti-cytochrome C monoclonal antibody (BD Biosciences, San Jose, CA, USA).

Determination of DNA fragmentation

After treatment, cells were harvested by scraping, washed twice with ice-cold PBS, and lysed in lysis buffer (10 mM Tris-HCl pH 8.0, 10 mM EDTA, and 0.2% Triton X-100) on ice for 20 min. After centrifugation, the supernatant was incubated with RNase A (200 μg/mL) at 37°C for 1 h, then incubated with proteinase K (1 mg/mL) with 1% SDS solution at 50°C for 2 h. The soluble DNA was extracted with phenol, ethanol precipitation, and resuspended in TE buffer. DNA was loaded on 1.5% agarose gel, which stained with ethidium bromide after migration.

Statistical analysis

Data in all experiments are represented as mean ± S.D. Statistical comparisons were carried out using two-tailed paired *t*-test. We considered $p<0.05$ (indicated * in figures) as significant. Analyses were carried out with Excel (Microsoft).

RESULTS

Paraquat induces apoptosis in NIH3T3 cells

Accumulation evidences indicate that paraquat lead to cell death by the induction of apoptosis (Han *et al*., 2014; Wang *et*

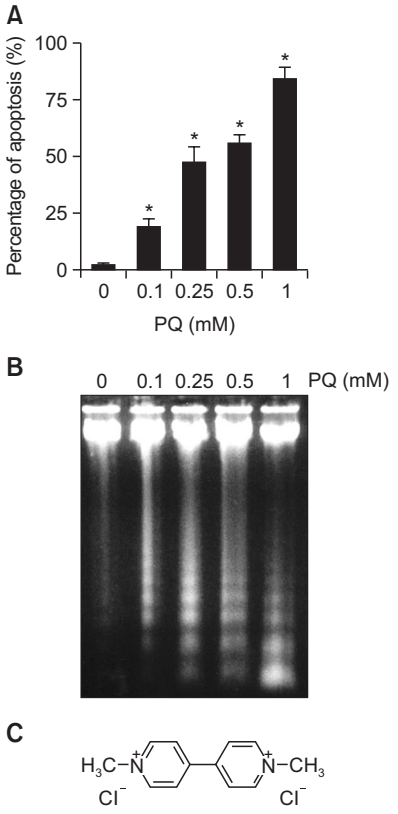

Fig. 1. Induction of apoptosis by paraquat in NIH3T3 cells. (A) NIH3T3 cells were treated with paraquat at final concentration indicated for 24 h. Cells were then stained with propidium iodide and apoptosis examined by flow cytometry. Each column shows the mean ± S.D. of triplicate experiments. * indicates a response that is significantly different from the control group as determined by two-tailed *t* test at $p<0.05$. (B) Cells were treated with different dose of paraquat for 24 h and DNA fragmentation was analyzed by 1.5% agarose gel electrophoresis. DNA bands were visualized by staining with ethidium bromide. (C) The chemical structure of paraquat.

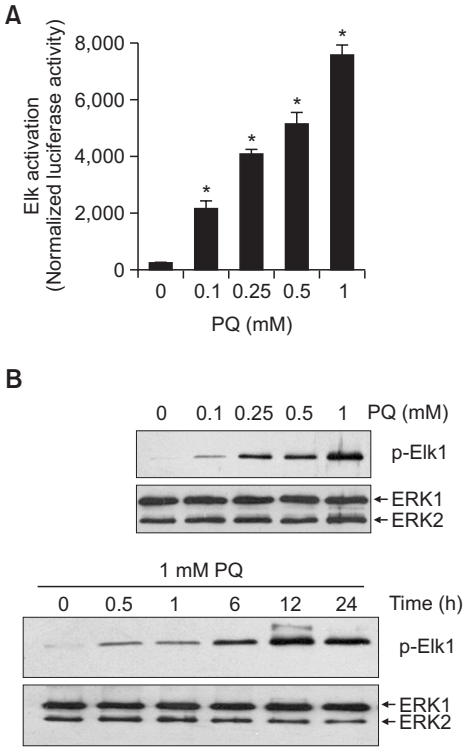

Fig. 2. The effect of paraquat on activation of ERK1/2 MAPKs in NIH3T3 cells. (A) Cells were cotransfected with GAL4-Elk/*firefly* luciferase vector and control *renilla* luciferase vector (pRL-Luc). Different dose of paraquat were then treated for 12 h. The cells were lysed, and luciferase activity was measured. *Firefly* luciferase reading was normalized to that or the control *renilla* luciferase. Results are shown as means ± S.D. (n=3). *<0.05. (B) Upper panel, cells were treated with the different dose of paraquat for 12 h. Lower panel, cells were treated with 1 mM paraquat for indicated time. Activation of ERK1/2 was determined by an immune complex kinase assay using Elk-1 fusion protein as substrate. ERK1/2-induced phosphorylation of Elk-1 was measures by immunoblotting with phosphor-Elk-1(Ser383) antibody. The ERK1/2 protein levels were shown using immunoblotting of ERK1/2 as control of immunocomplex.

al., 2014c). Although several prior studies have investigated the mechanism of paraquat-induced apoptosis, however, it is not fully understood. In the present study, we therefore attempted to investigate the mechanism of paraquat-induced apoptosis using NIH3T3 cells. After exposure to 0.1, 0.25, 0.5, or 1 mM paraquat, sub-G_1 DNA content and DNA fragmentation were evaluated in NIH3T3 cells. Fig. 1A showed that paraquat caused apoptosis of NIH3T3 cells in a dose-dependent manner, with a concentration of 1 mM paraquat resulting in death of greater than 80% of the cell population by 24 h of treatment. The intensity of paraquat-induced DNA ladders increased with increasing dose of paraquat in NIH3T3 cells (Fig. 1B). These data indicate that paraquat is able to induce apoptosis in a dose-dependent manner in NIH3T3 cells.

ERK signaling pathway contributes to paraquat-induced apoptosis

It is well established that MAPK signaling pathway mediates stress induced apoptosis (Kumar *et al*., 2014; Wang *et al*., 2014b). Therefore, we further analyzed the relation of MAPK signal in paraquat-induced apoptosis. We first investigated whether paraquat treatment led to ERK activation. NIH3T3 cells were cotransfected with Gal4-Elk1-*firefly* luciferase vector, which contains the Gal4 DNA binding domain fused to the Elk-1 carboxyl-terminal transactivation domain, and pRL-Luc, which contains the *renilla* luciferase gene, and then fresh medium containing different dose of paraquat was then added to cells. The cells were harvested 12 h later, and the luciferase activities were determined using a luminometer. Elk1 is a transcriptional factor that is activated in response to activation of mitogen activated protein kinase (MAPK) and the *renilla* luciferase plasmid (pRL-Luc) was used to normalize the transfection efficiency. As shown in Fig. 2A, luciferase activity was elevated by treatment of 0.1 mM paraquat and increased in a dose-dependent manner. To confirm the phosphorylation of ERK by paraquat, NIH3T3 cells were exposed to different dose of paraquat for various lengths of time, and ERK activity was the assessed using immunocomplex kinase assay, that is measurement of its phosphorylation by Western blot analysis with anti-phospho Elk-1 antibody. Total ERK protein

levels were monitored using antibody capable of recognizing unphosphorylated forms of the proteins. As shown in Fig. 2B, 1 mM paraquat, which resulted in significant apoptosis, led to strong activation of ERK. Activation was apparent at about 30 min following treatment with 1 mM paraquat and persisted for at least 24 h.

To evaluate the functional consequence of ERK activation in paraquat-induced apoptosis, we used commercially available MEK1/2 inhibitory compound U0126, which are highly selective in its inhibition of ERK pathway. We observed that pretreatment of NIH3T3 cells with 20 μM U0126 totally abolished ERK phosphorylation in response to paraquat treatment (Fig. 3, right panel). Paraquat-induced apoptosis was significantly reduced when cells were pretreated with U0126 for 30 min prior to addition of 1 mM paraquat, and this protective effect of the MEK inhibitors was dose-dependent and occurred with doses expected to suppress ERK activation (Fig. 3, left panel).

JNK and p38 MAPK signaling pathway are not related with paraquat-induced apoptosis

JNK (c-Jun N-terminal kinase) and p38 have been implicated in stress-related responses and the induction of apoptosis. Therefore, we investigated whether JNK and p38 involved in the induction of paraquat-induce apoptosis. To compare the patterns of activation of the JNK and p38 pathways in response to paraquat in NIH3T3 cells, cells were cotransfected with either Gal4-c-Jun-*firefly* luciferase vector for measuring JNK activation, or Gal4-CHOP-*firefly* luciferase vector for measuring p38 kinase activation and pRL-Luc following exposure to different dose of paraquat for 12 h, and then cells were harvested and luciferase activities were measured. The results, shown in Fig. 4A, B, demonstrated that both p38 and JNK were activated in response to paraquat treatment. To investigate the functional consequences of p38 and JNK activation, paraquat-induced apoptosis after prevention of JNK and p38 was measured. NIH3T3 cells were pretreated with p38 specific inhibitor, SB203580 or transiently transfected with 0.2 μM each antisense JNK1 and JNK2 oligonucleotides (JNK1+JNK2AS), which was phosphorothioate oligonucleotides targeted to JNK1 and JNK2 mRNA to block JNK/SPAK pathway. As shown in Fig. 4C, the JNK1+JNK2AS-transfecting NIH3T3 cells and the treatment of cells with SB203580 during exposure to paraquat did not prevent paraquat-induced apoptosis. These results indicate that although JNK and p38 were activated in response to paraquat, neither JNK nor p38 plays a role in regulating paraquat-induced apoptosis of NIH cells. Taken together, among of the three MAPKs, only ERK appears to play a major role in influencing the survival of paraquat-treated NIH3T3 cells.

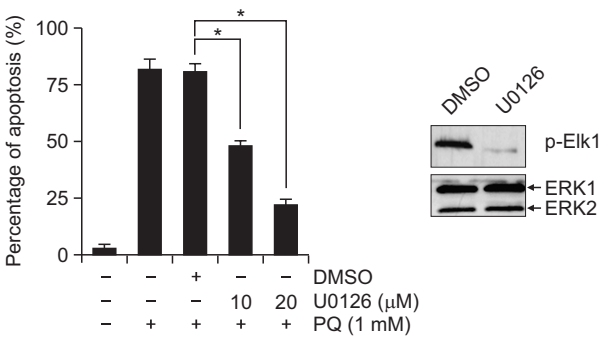

Fig. 3. Inhibition of induction of apoptosis in NIH3T3 cells exposed to paraquat after pretreatment with the MEK inhibitor, U0126. Left panel, percentage of apoptotic cells was shown using PI staining. Results are shown as means ± S.D. (n=3). *<0.05. Right panel, inhibition of ERK1/2 activation by 20 μM U0126 was determined as described in Fig. 2B.

ERK MAPK is mediated with release of cytochrome C in paraquat-treated cells

Apoptosis have been described in two major pathways. One pathway is extrinsic apoptosis pathway by external receptor-dependent stimuli. The ligands, such as FASL, TRAIL or TNF, interact with their receptors, and then adaptor molecule, FADD (Fas-associated death domain protein), is associated with death receptors, and subsequently activates caspase-8 leading to activation of downstream effector caspases, thus inducing apoptosis (Lavrik and Krammer, 2012; Nikoletopoulou *et al*., 2013). The second pathway is intrinsic apoptosis pathway that is mitochondria-dependent and results

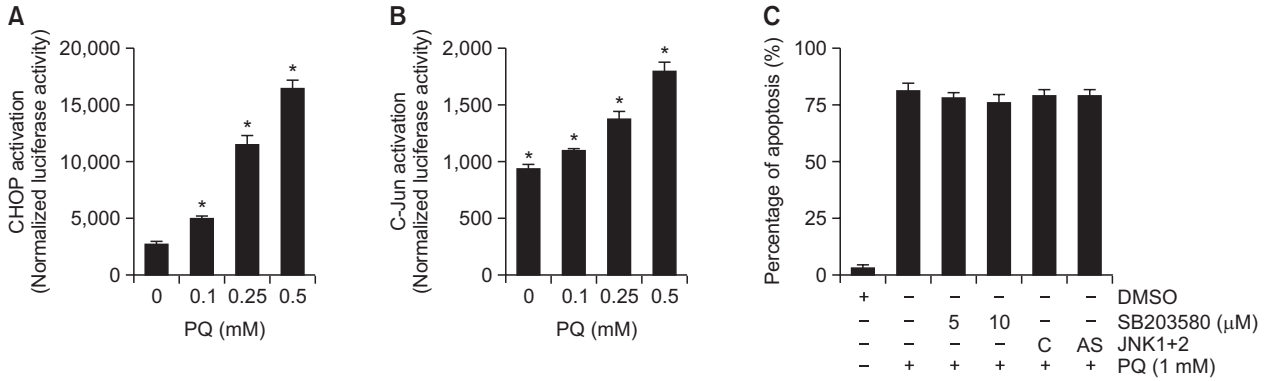

Fig. 4. The effect of paraquat on activation of JNK and p38 MAPKs. NIH3T3 cells were cotransfected with either Gal4-CHOP trans-reporting system (A) or GAL4-c-Jun trans-reporting system (B) and pRL-Luc, and then cells were treated with different dose of paraquat for 12 h. The luciferase activity was measured as described in Fig. 2A. Results are shown as means ± S.D. (n=3). *<0.05. (C) Cells were preincubated with p38 inhibitors SB203580, or transiently transfected with a combination of JNK1 and JNK2 antisense oligonucleotides (AS) or control oligonuleotide (C), and subsequently treated with 1 mM paraquat for 24 h, and then the extent of apoptosis was measured.

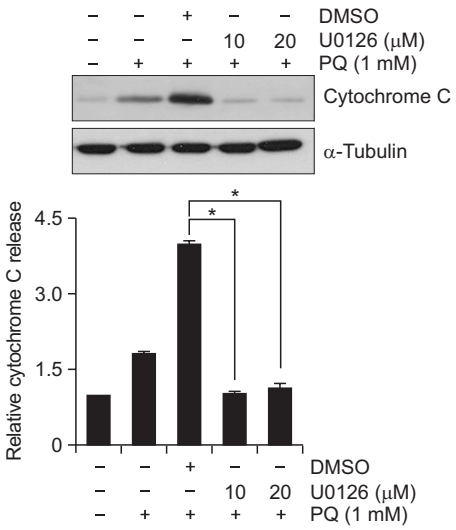

Fig. 5. Suppression of cytochrome C release by MEK inhibitor. Cells were pretreated with the U0126 (20 μM) for 30 min and then treated with 1 mM paraquat for 24 h. Upper panel, the cytosolic fraction was separated from mitochondria-enriched fraction and subjected to Western blot analysis with a monoclonal antibody to cytochrome C. Lower panel, the amount of cytochrome C release was quantified by densitometry and corrected for the amount of α-Tubulin in the corresponding lysate. Results are shown as means ± S.D. (n=3). *<0.05.

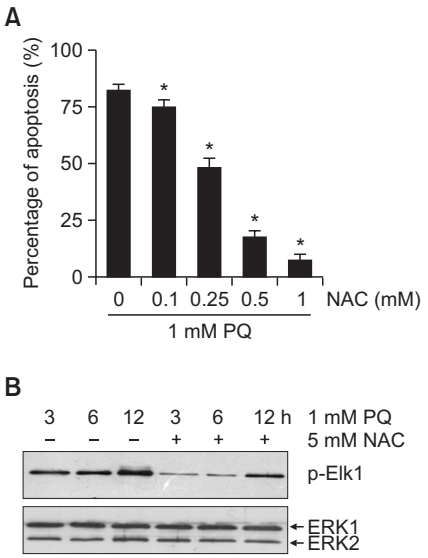

Fig. 6. The effect of ROS on the activation of ERK1/2 induced by paraquat in NIH3T3 cells. (A) NIH3T3 cells were pretreated with different dose of NAC for 12 h and then treated with 1 mM paraquat. The extent of apoptosis was measured 24 h later. Results are shown as means ± S.D. (n=3). *<0.05. (B) Cells were treated with 1 mM paraquat for indicated time in the presence or absence of 5 mM NAC, and activity of ERK1/2 was determined as described in Fig. 2B.

from release of cytochrome C leading to caspase-9 activation through the apoptotic protease-activating factor-1 (Apaf-1) (Huttemann *et al*., 2011; Landes and Martinou, 2011; Monian and Jiang, 2012). Therefore, we sought to investigate whether cytochrome C release occurred in response to paraquat treatment, and if so, to determine whether it was dependent on ERK activation. We isolated cytosolic fractions from lysates of NIH3T3 cells treated with paraquat for 24 h in the presence or absence of U0126 (20 μM). Western blot analysis revealed accumulation of cytosolic cytochrome C in paraquat-induced apoptosis (Fig. 5). Importantly, this process was markedly inhibited in the presence of the MEK inhibitors, U0126, suggesting that ERK activation is required for paraquat-induced cytochrome C release (Fig. 5). In the present studies, we did not observe any change in either Fas or FasL expression in paraquat-treated NIH3T3 cells (data not shown). We did, however, observe increased levels of cytochrome C in the cytoplasm of paraquat-treated cells relative to untreated cells. These results suggest that cytochrome C release play a role in mediating paraquat-induced apoptosis. The ability of the MEK inhibitors to diminish this effect suggests that the ERK signaling pathway functions upstream of cytochrome C release in the paraquat-induced apoptosis.

Intracellular ROS production by paraquat requires activation of ERK1/2

Recent evidence has suggested that ROS stimulate MAPK activities including ERK, p38 and JNK, which are key events in many cellular processes (Nikoletopoulou *et al*., 2013; Son *et al*., 2013). Therefore, intracellular ROS production by paraquat treatment was examined to determine whether or not it led to ERK activation, which could be involved in the paraquat-induced apoptosis. To test this possibility, the level of intracellular ROS production in response to paraquat was investigated using DCFHDA. We found that paraquat treatment led to significantly increase the intracellular ROS production, which could be completely blocked by treatment with 5 mM N-acetylcysteine (NAC) (data not shown). To further investigate the enhancement of ROS production by paraquat is involved in the induction of apoptosis, NIH3T3 cells were pretreated with NAC for 12 h. Subsequently, the cells were incubated with 1 mM of paraquat for an additional 24 h, and stained with propidium iodide, and the level of apoptosis was measured by FACsan flow cytometry. The data presented in Fig. 6A shows that NAC was able to significantly prevent paraquat-induced apoptosis, suggesting that intracellular ROS production is required for paraquat-induced apoptosis in NIH3T3 cells.

We next investigated whether the intracellular ROS production induced by paraquat could stimulate ERK activation. The NIH3T3 cells were pretreated with NAC for 12 h and the medium was replaced with fresh medium in the presence or absence of 1 mM paraquat and the ERK activity was measured. The results, shown in Fig. 6B, demonstrated that the inhibition of intracellular ROS generation using 5 mM NAC led to markedly decrease in paraquat activation of ERK, suggesting that intracellular ROS, which was produced by paraquat, contributes to the ERK activation in the NIH3T3 cells.

DISCUSSION

Many studies have reported that paraquat was a potent inducer of intracellular ROS, which have a critical role in paraquat-induced cell death. In addition to ROS modulate many downstream signaling pathway, including NF-κB, p38 MAPK and mitochondrial pathway (Nahirnyj *et al*., 2013; Han *et al*.,

2014; Wang *et al*., 2014a; Wang *et al*., 2014c). However, the mechanisms of the paraquat-induced apoptosis through ROS generation remain to be resolved. In our present study, we were sought to elucidate the mechanism of paraquat-induced apoptosis, including MAPK and mitochondria pathway. We found that paraquat induced activity of ERK1/2, p38 and JNK MAPKs, but only ERK MAPK was related with paraquat-induced apoptosis. Moreover, ERK1/2 MAPK, which is play a role in cell survival, was surprisingly mediated with ROS generation and cytochrome C release in paraquat-treated NIH3T3 cells.

The importance of MAPK signaling pathways in regulating apoptosis during conditions of stress has been widely investigated. Many prior studies have provided evidence indicating that the ERK1/2 pathway is regulated mostly by mitogenic stimuli, and leads to the production of proteins required for cell growth and differentiation (Craig *et al*., 2008; Kim and Choi, 2010; Munshi and Ramesh, 2013). However, more recently, several studies have demonstrated that inhibition of ERK signaling leads to increased sensitivity of anticancer drug (Ohmichi *et al*., 2005; Tian *et al*., 2014a; Tian *et al*., 2014b). ERK activation induces the deveplopment of B cell (Gold, 2008) and activation of ERK is also involved in the inducation of apoptosis in neuronal and various cancer cells (Agrawal *et al*., 2014; Deschenes-Simard *et al*., 2014; Esmaeili *et al*., 2014). Such differential effects of ERK pathway could reflect cell type- and extracellular stress-specificity. In the present studies using NIH3T3 cells, we have provided evidence that activation of ERK is important for the induction of paraquat-induced apoptosis in NIH3T3 cells. Paraquat treatment resulted in high and sustained activation of ERK in these cells. We also found that down-regulation of ERK led to an inhibition of paraquat-induced apoptosis.

In summary, paraquat treatment led to apoptosis, which was associated with release of cytochrome C from the mitochondria, and increase ERK1/2 activity. In addition, the MEK specific inhibitor, U0126, was quite effective in protecting NIH3T3 cells against paraquat-mediated apoptosis. The correlation of removing intracellular ROS with increased cell survival as well as decreased ERK activity after exposure to paraquat suggest that raising the intracellular ROS induced by paraquat stimulates ERK activation, which may, at least in part, involve in the paraquat-induced apoptosis in NIH3T3 cells. Identification of the downstream target of the ROS-cascade in the paraquat-signaling pathway will require additional study. Characterization of this pathway will contribute to the understanding about important signaling pathway of paraquat-induced apoptosis, which will lead to the development of specifically targeted drugs to achieve attenuated paraquat toxicity.

ACKNOWLEDGMENTS

This research was supported by a grant [NRF-2011-0029629 and NRF-2013M2B2A9A03051397] from the Ministry of Education, Science and Technology, the Korean government.

CONFLICT OF INTEREST

None declared.

REFERENCES

Agrawal, M., Bhaskar, A. S. and Rao, P. V. (2014) Involvement of mitogen-activated protein kinase pathway in T-2 toxin-induced cell cycle alteration and apoptosis in human neuroblastoma cells. *Mol. Neurobiol.* Aug 2. [Epub ahead of print]

Bost, F., McKay, R., Dean, N. and Mercola, D. (1997) The JUN kinase/stress-activated protein kinase pathway is required for epidermal growth factor stimulation of growth of human A549 lung carcinoma cells. *J. Biol. Chem.* **272**, 33422-33429.

Chang, X., Lu, W., Dou, T., Wang, X., Lou, D., Sun, X. and Zhou, Z. (2013) Paraquat inhibits cell viability via enhanced oxidative stress and apoptosis in human neural progenitor cells. *Chem. Biol. Interact.* **206**, 248-255.

Craig, E. A., Stevens, M. V., Vaillancourt, R. R. and Camenisch, T. D. (2008) MAP3Ks as central regulators of cell fate during development. *Dev. Dyn.* **237**, 3102-3114.

Darling, N. J. and Cook, S. J. (2014) The role of MAPK signalling pathways in the response to endoplasmic reticulum stress. *Biochim. Biophys. Acta* **1843**, 2150-2163.

Deschenes-Simard, X., Kottakis, F., Meloche, S. and Ferbeyre, G. (2014) ERKs in cancer: friends or foes? *Cancer Res.* **74**, 412-419.

Ding, H. D., Zhang, X. H., Xu, S. C., Sun, L. L., Jiang, M. Y., Zhang, A. Y. and Jin, Y. G. (2009) Induction of protection against paraquat-induced oxidative damage by abscisic acid in maize leaves is mediated through mitogen-activated protein kinase. *J. Integr. Plant Biol.* **51**, 961-972.

Esmaeili, M. A., Farimani, M. M. and Kiaei, M. (2014) Anticancer effect of calycopterin via PI3K/Akt and MAPK signaling pathways, ROS-mediated pathway and mitochondrial dysfunction in hepatoblastoma cancer (HepG2) cells. *Mol. Cell. Biochem.* **397**, 17-31

Fei, Q. and Ethell, D. W. (2008) Maneb potentiates paraquat neurotoxicity by inducing key Bcl-2 family members. *J. Neurochem.* **105**, 2091-2097.

Fei, Q., McCormack, A. L., Di Monte, D. A. and Ethell, D. W. (2008) Paraquat neurotoxicity is mediated by a Bak-dependent mechanism. *J. Biol. Chem.* **283**, 3357-3364.

Giordano, S., Darley-Usmar, V. and Zhang, J. (2014) Autophagy as an essential cellular antioxidant pathway in neurodegenerative disease. *Redox Biol.* **2**, 82-90.

Gold, M. R. (2008) B cell development: important work for ERK. *Immunity* **28**, 488-490.

Haberzettl, P. and Hill, B. G. (2013) Oxidized lipids activate autophagy in a JNK-dependent manner by stimulating the endoplasmic reticulum stress response. *Redox Biol.* **1**, 56-64.

Han, J., Zhang, Z., Yang, S., Wang, J., Yang, X. and Tan, D. (2014) Betanin attenuates paraquat-induced liver toxicity through a mitochondrial pathway. *Food Chem. Toxicol.* **70**, 100-106.

Hong, G. L., Liu, J. M., Zhao, G. J., Wang, L., Liang, G., Wu, B., Li, M. F., Qiu, Q. M. and Lu, Z. Q. (2013) The reversal of paraquat-induced mitochondria-mediated apoptosis by cycloartenyl ferulate, the important role of Nrf2 pathway. *Exp. Cell Res.* **319**, 2845-2855.

Huttemann, M., Pecina, P., Rainbolt, M., Sanderson, T. H., Kagan, V. E., Samavati, L., Doan, J. W. and Lee, I. (2011) The multiple functions of cytochrome c and their regulation in life and death decisions of the mammalian cell: From respiration to apoptosis. *Mitochondrion* **11**, 369-381.

Kim, D., Koo, J. S. and Lee, S. (2014) Overexpression of reactive oxygen species scavenger enzymes is associated with a good prognosis in triple-negative breast cancer. *Oncology* **88**, 9-17.

Kim, E. K. and Choi, E. J. (2010) Pathological roles of MAPK signaling pathways in human diseases. *Biochim. Biophys. Acta* **1802**, 396-405.

Kumar, P., Rao, G. N., Pal, B. B. and Pal, A. (2014) Hyperglycemia-induced oxidative stress induces apoptosis by inhibiting PI3-kinase/Akt and ERK1/2 MAPK mediated signaling pathway causing down-regulation of 8-oxoG-DNA glycosylase levels in glial cells. *Int. J. Biochem. Cell Biol.* **53**, 302-319.

Landes, T. and Martinou, J. C. (2011) Mitochondrial outer membrane permeabilization during apoptosis: the role of mitochondrial fission. *Biochim. Biophys. Acta* **1813**, 540-545.

Lavrik, I. N. and Krammer, P. H. (2012) Regulation of CD95/Fas signal-

ing at the DISC. *Cell Death Differ.* **19**, 36-41.
Li, J., O, W., Li, W., Jiang, Z. G. and Ghanbari, H. A. (2013) Oxidative stress and neurodegenerative disorders. *Int. J. Mol. Sci.* **14**, 24438-24475.
Lim, N. R., Thomas, C. J., Silva, L. S., Yeap, Y. Y., Yap, S., Bell, J. R., Delbridge, L. M., Bogoyevitch, M. A., Woodman, O. L., Williams, S. J., May, C. N. and Ng, D. C. (2013) Cardioprotective 3',4'-dihydroxyflavonol attenuation of JNK and p38(MAPK) signalling involves CaMKII inhibition. *Biochem. J.* **456**, 149-161.
Liu, P., Kong, F., Wang, J., Xu, H., Qi, T. and Meng, J. (2014) Involvement of IGF-1 and MEOX2 in PI3K/Akt1/2 and ERK1/2 pathways mediated proliferation and differentiation of perivascular adipocytes. *Exp. Cell. Res*. Sep 18. pii: S0014-4827 (14)00400-5. doi: 10.1016/j.yexcr.2014.09.011. [Epub ahead of print]
Mak, S. K., Tewari, D., Tetrud, J. W., Langston, J. W. and Schule, B. (2011) Mitochondrial dysfunction in skin fibroblasts from a Parkinson's disease patient with an alpha-synuclein triplication. *J. Parkinsons Dis.* **1**, 175-183.
Meierjohann, S. (2014) Oxidative stress in melanocyte senescence and melanoma transformation. *Eur. J .Cell Biol.* **93**, 36-41.
Miller, R. L., Sun, G. Y. and Sun, A. Y. (2007) Cytotoxicity of paraquat in microglial cells: Involvement of PKCdelta- and ERK1/2-dependent NADPH oxidase. *Brain Res.* **1167**, 129-139.
Monian, P. and Jiang, X. (2012) Clearing the final hurdles to mitochondrial apoptosis: regulation post cytochrome C release. *Exp. Oncol.* **34**, 185-191.
Munshi, A. and Ramesh, R. (2013) Mitogen-activated protein kinases and their role in radiation response. *Genes Cancer* **4**, 401-408.
Nahirnyj, A., Livne-Bar, I., Guo, X. and Sivak, J. M. (2013) ROS detoxification and proinflammatory cytokines are linked by p38 MAPK signaling in a model of mature astrocyte activation. *PLoS One* **8**, e83049.
Nikoletopoulou, V., Markaki, M., Palikaras, K. and Tavernarakis, N. (2013) Crosstalk between apoptosis, necrosis and autophagy. *Biochim. Biophys. Acta* **1833**, 3448-3459.
Ohmichi, M., Hayakawa, J., Tasaka, K., Kurachi, H. and Murata, Y. (2005) Mechanisms of platinum drug resistance. *Trends Pharmacol. Sci.* **26**, 113-116.
Prakash, J., Yadav, S. K., Chouhan, S. and Singh, S. P. (2013) Neuroprotective role of Withania somnifera root extract in maneb-paraquat induced mouse model of parkinsonism. *Neurochem. Res.* **38**, 972-980.
Qin, X., Wu, Q., Lin, L., Sun, A., Liu, S., Li, X., Cao, X., Gao, T., Luo, P., Zhu, X. and Wang, X. (2014) Soluble epoxide hydrolase deficiency or inhibition attenuates MPTP-induced parkinsonism. *Mol. Neurobiol.* Aug 17. [Epub ahead of print]
Rincheval, V., Bergeaud, M., Mathieu, L., Leroy, J., Guillaume, A., Mignotte, B., Le Floch, N. and Vayssiere, J. L. (2012) Differential effects of Bcl-2 and caspases on mitochondrial permeabilization during endogenous or exogenous reactive oxygen species-induced cell death: a comparative study of H(2)O(2), paraquat, t-BHP, etoposide and TNF-alpha-induced cell death. *Cell Biol.Toxicol.* **28**, 239-253.
Son, Y., Kim, S., Chung, H. T. and Pae, H. O. (2013) Reactive oxygen species in the activation of MAP kinases. *Methods Enzymol*. **528**, 27-48.
Tian, F., Dong, L., Zhou, Y., Shao, Y., Li, W., Zhang, H. and Wang, F. (2014a) Rapamycin-Induced apoptosis in HGF-stimulated lens epithelial cells by AKT/mTOR, ERK and JAK2/STAT3 pathways. *Int. J. Mol. Sci.* **15**, 13833-13848.
Tian, H., Zhang, D., Gao, Z., Li, H., Zhang, B., Zhang, Q., Li, L., Cheng, Q., Pei, D. and Zheng, J. (2014b) MDA-7/IL-24 inhibits Nrf2-mediated antioxidant response through activation of p38 pathway and inhibition of ERK pathway involved in cancer cell apoptosis. *Cancer Gene Ther.* Sep 19. doi: 10.1038/cgt.2014.45. [Epub ahead of print]
Tormos, A. M., Talens-Visconti, R., Nebreda, A. R. and Sastre, J. (2013) p38 MAPK: a dual role in hepatocyte proliferation through reactive oxygen species. *Free Radic. Res.* **47**, 905-916.
Wallace, M. A., Bailey, S., Fukuto, J. M., Valentine, J. S. and Gralla, E. B. (2005) Induction of phenotypes resembling CuZn-superoxide dismutase deletion in wild-type yeast cells: an in vivo assay for the role of superoxide in the toxicity of redox-cycling compounds. *Chem. Res. Toxicol.* **18**, 1279-1286.
Wang, F., Franco, R., Skotak, M., Hu, G. and Chandra, N. (2014a) Mechanical stretch exacerbates the cell death in SH-SY5Y cells exposed to paraquat: mitochondrial dysfunction and oxidative stress. *Neurotoxicology* **41**, 54-63.
Wang, J., Deng, X., Zhang, F., Chen, D. and Ding, W. (2014b) ZnO nanoparticle-induced oxidative stress triggers apoptosis by activating JNK signaling pathway in cultured primary astrocytes. *Nanoscale Res. Lett.* **9**, 117.
Wang, X., Luo, F. and Zhao, H. (2014c) Paraquat-induced reactive oxygen species inhibit neutrophil apoptosis via a p38 MAPK/NF-kappaB-IL-6/TNF-alpha positive-feedback circuit. *PLoS One* **9**, e93837.